Journal of Smart Sensor and Materials
Volume 1, 2023, No 4 (2023)

SIMULATION OF INTERDIGITATED ARRAY WITH COUNTER ELECTRODE IN SHALLOW ELECTROCHEMICAL CELL

Cristian F. Guajardo Yévenes[1,2,*] and Werasak Surareungchai[3,4]

[1]Biological Engineering Program, Faculty of Engineering, King Mongkut's University of Technology Thonburi, 49 Soi Thian Thale 25, Thanon Bang Khun Thian Chai Thale Bangkok 10150, THAILAND
[2]Pilot Plant Development and Training Institute, King Mongkut's University of Technology Thonburi, 49 Soi Thian Thale 25, Thanon Bang Khun Thian Chai Thale Bangkok 10150, THAILAND
[3]Nanoscience and Nanotechnology Graduate Program, King Mongkut's University of Technology Thonburi, 49 Soi Thian Thale 25, Thanon Bang Khun Thian Chai Thale Bangkok 10150, THAILAND
[4]School of Bioresources and Technology, King Mongkut's University of Technology Thonburi, 49 Soi Thian Thale 25, Thanon Bang Khun Thian Chai Thale Bangkok 10150, THAILAND
[*]*Corresponding author: cristian.gua@kmutt.ac.th*

ABSTRACT

Interdigitated array of electrodes (IDAE) is a popular configuration for many sensors and transducers, including microfluidic electrochemical cells. Due to the difficulty of obtaining analytical equations for IDAEs in shallow electrochemical cells, numerical simulations are commonly performed. In particular, most of these simulations don't include a counter electrode, since this is normally not the electrode of interest, or avoid to include it, because its potential and concentrations are unknown until the cell is experimentally potentiostated. In this research, the problem of unknown concentrations at the counter electrode is addressed by using a property of coplanar electrodes, which states that the average concentration at the plane of the electrodes does not change in time and equals the initial bulk concentration. This leads to obtain an additional boundary condition for the counter electrode, which allows the numerical calculation of collection efficiency (indicator of performance of the IDAE), and which is normally not possible when the counter electrode is not included in the simulation domain. Steady-state currents and collection efficiencies were computed for several cases of cell heights, showing that there is a compromise between sensitivity (current) and performance (collection efficiency) as the cell becomes shallower.

Keywords: shallow electrochemical cells, interdigitated arrays, numerical simulation, counter electrode, collection efficiency.

INTRODUCTION

Interdigitated array of electrodes (IDAE) is a popular configuration for many sensors and transducers [1]. Among these, microfluidic devices are frequently equipped with IDAEs for electrochemical sensing, because of their sensitivity and compatibility with microfabrication techniques [2, 3].

Due to the difficulty of obtaining analytical equations for describing IDAEs in shallow electrochemical cells, numerical simulations are commonly performed during the phases of design or assessment of performance of such devices. In particular, most of these simulations don't include a counter electrode [4, 5], since this is normally not the electrode of interest, or avoid to include it [6, 7], because its potential is unknown until the cell is experimentally potentiostated (unlike the working electrodes, whose potentials

are known *a priori*).

When the number of bands in the IDAE is very large (infinite), and the counter electrode is very far (infinitely), it is possible to simulate the electrochemical cell without a counter electrode [4, 5]. In this case, the steady-state current generated at one array is completely collected by the other array (100% collection efficiency) [8]. In practice, it is known that even for large number of bands and far counter electrode, the collection efficiency is not 100% [6–8]. However, this simplified model allows fairly precise calculation of the current generated at the IDAE, at the expense of making impossible to calculate collection efficiencies, which is an important indicator of performance of IDAEs.

This problem can be partially solved when considering a finite number of bands and a counter electrode placed infinitely far from the IDAE. In this case, the boundary condition for the counter electrode is replaced by bulk concentration far from the IDAE [6, 7]. This approach leads to models for simulations which can predict different currents at both arrays of the IDAE, meaning that the current generated at one array cannot be completely collected at the other (collection efficiency < 100%). In this case, the species that cannot be collected by the IDAE diffuses to the region of bulk concentration.

However, the problem with this last approach is that in some practical cases there are restrictions of space, and the counter electrode must necessarily be placed close to the IDAE [9]. This forces to model the counter electrode inside the simulation domain, and therefore it is no longer possible to use a boundary condition of bulk concentration as a replacement for that of the counter electrode.

In this research, the problem of unknown concentrations at the counter electrode is addressed by using a property of coplanar electrodes, which states that the average concentration at the plane of the electrodes does not change in time and equals the initial bulk concentration [10]. This leads to obtain an additional boundary condition for the counter electrode, which allows the numerical calculation of collection efficiency when the counter electrode is included in the simulation domain. Steady-state currents and collection efficiencies were computed for several cases of cell height, which showed that higher currents can be obtained at the expense of lower collection efficiencies when the cell is tall, while higher collection efficiencies can be obtained at the expense of lower currents when the cell is shallow.

MATERIALS AND METHODS

Model of the IDEA

Consider an IDAE located at the bottom of an electrochemical cell of height H (Figure 1). The IDAE consists of two arrays, A (black) and B (gray), of N_A and N_B bands each. Consecutive bands are separated by a distance W between their centers, have width of w_A and w_B, and share a common length L, which is in contact with the electrochemical solution. The electrochemical cell also includes a counter electrode C, which is placed at a distance of w_G from the IDAE. This configuration is driven by a bipotentiostat, such that each of the arrays can be potentiostated independently.

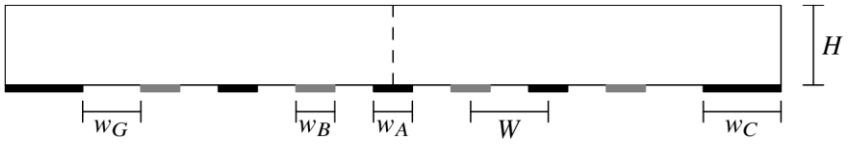

Figure 1. Shallow electrochemical cell containing an IDAE with counter electrode placed in close proximity. In this work the number of bands for the arrays *A* and *B* is given by the relation $N_A + 1 = N_B = 4$, and the counter electrode *C* is split in two parts (located at the left and right of the cell) in order to make the whole cell symmetric with respect to its center.

Inside the cell, there is a solution consisting of a mixture of oxidized (*O*) and reduced (*R*) species, of uniform initial concentrations $c_{O,i}$ and $c_{R,i}$ respectively, which are transported only by diffusion (with diffusion coefficient *D*) and react at the surface of the electrodes by exchanging n_e electrons

$$O + n_e\, e^- \rightleftharpoons R \tag{1}$$

For the sake of simplicity, reversible electrode reactions are assumed, and therefore, Nernst equation is valid even when current flows through the electrodes [11].

In order to reduce the problem to two dimensions, we considered that the length *L* is sufficiently large, such that fringing effects at the ends of each band can be neglected. Additionally, we made the cell symmetric by considering the number of bands for each array such that $N_B = N_A + 1$, and by splitting the counter electrode in two equal parts (located at the left and right of the cell) each having a width of w_C (Figure 1). Under these conditions, only half cell is sufficient for modeling the concentration profile, which is given by the two-dimensional diffusion equation

$$\frac{1}{D}\frac{\partial c_\sigma}{\partial t} = \frac{\partial^2 c_\sigma}{\partial x^2} + \frac{\partial^2 c_\sigma}{\partial z^2} \tag{2a}$$

where $c_\sigma(x, z, t)$ is the concentration of species σ (either *O* or *R*), which is subject to the initial concentrations

$$c_\sigma(x, z, 0^-) = c_{\sigma,i} \tag{2b}$$

as well as boundary conditions for insulation (top, bottom, right and left walls), symmetry (axis at the center) and applied concentrations c_σ^A and c_σ^B at the bands *A* and *B* respectively.

Due to the assumption of reversible electrode reactions, the concentrations on any electrode *E* (either array *A*, array *B* or *C*) are uniform. This is due to a combination of Nernst equation:

$$ln\left(\frac{c_O^E}{c_R^E}\right) = \frac{Fn_e}{RT}(V_E - V^{o\prime}) \tag{2c}$$

(where *F* is Faraday's constant, *R* is the universal gas constant, *T* is the temperature of the system, V_E is the potential at the electrode *E*, and $V^{o\prime}$ is the formal potential of the redox

couple) and the fact that the sum of concentrations at any point in the cell is constant and uniform [10]

$$c_O(x,z,t) + c_R(x,z,t) = c_{O,i} + c_{R,i} \tag{2d}$$

Also, both conditions make the concentrations of species *O* and *R* on each electrode *E* (either array *A*, array *B* or *C*) dependent only on the potential at that same electrode

$$c_O^E = \frac{c_{O,i} + c_{R,i}}{1 + e^{\frac{-Fn_e}{RT}(V_E - V^{o\prime})}} \tag{3a}$$

$$c_R^E = \frac{c_{R,i} + c_{O,i}}{1 + e^{\frac{+Fn_e}{RT}(V_E - V^{o\prime})}} \tag{3b}$$

The only remaining boundary condition to be known is that of the counter electrode. In practice, the potential at the counter electrode is not known in advance (as well as its concentrations), because this is adjusted automatically by the bipotentiostat as the experiment progresses. However, with the property of average concentrations [10]

$$\int_{cell} c_\sigma(x,z,t) - c_{\sigma,i} dx = 0 \quad \text{for all } (z, t) \tag{4}$$

it is possible to derive an expression for the concentrations at the counter electrode. This property states that the average concentration of species σ (along any horizontal line in the cell) is constant and equals its initial concentration when the net current entering the whole cell is zero (Kirchhoff's current law is satisfied). This corresponds to a special case of the continuity equation (in its integral form), which states that the total amount of species in a fixed volume doesn't change when there is no net flux of species into the volume. This property leads to the following boundary condition at one half of the counter electrode

$$c_\sigma^C = c_{\sigma,i} - \frac{1}{w_C} \int_{\text{outside}C} c_\sigma(x,0,t) - c_{\sigma,i} dx \tag{5}$$

After the concentration profile is known, the current at the electrode *E* (array *A*, array *B* or *C*) is obtained by integrating on its surface

$$i_E = \int_E \mp F\, n_e D \frac{\partial c_\sigma}{\partial z}(x,0,t) L dx \tag{6}$$

where minus or plus signs should be used when the species σ corresponds to *O* or *R* respectively.

Implementation of the simulations

All equations were normalized by using the relations $\gamma_\sigma = [c_\sigma - c_\sigma^A]/[c_\sigma^B - c_\sigma^A]$, $\xi = x/W$, $\zeta = z/W$ and $\tau = \pi^2 Dt/W^2$, which transformed the diffusion equation, its initial concentration and the concentrations on the electrodes into

$$\pi^2 \frac{\partial \gamma_\sigma}{\partial \tau} = \frac{\partial^2 \gamma_\sigma}{\partial \xi^2} + \frac{\partial^2 \gamma_\sigma}{\partial \zeta^2} \tag{7a}$$

$$\gamma_\sigma(\xi, \zeta, 0^-) = \gamma_{\sigma,i} = \frac{c_{\sigma,i} - c_\sigma^A}{c_\sigma^B - c_\sigma^A} \tag{7b}$$

$$\gamma_\sigma(\xi, 0, \tau) = 0 \text{ for } \xi \in A \tag{7c}$$

$$\gamma_\sigma(\xi, 0, \tau) = 1 \text{ for } \xi \in B \tag{7d}$$

$$\gamma_\sigma^C = \gamma_{\sigma,i} - \frac{1}{w_C/W} \int_{\text{outside}C} \gamma_\sigma(\xi, 0, \tau) - \gamma_{\sigma,i} d\xi \tag{7e}$$

while the boundary conditions for insulation and symmetry remained equal to zero. Finally, the normalization of the current at the electrode E (array A, array B or C) resulted in

$$\frac{i_E/L}{\pi^2 F n_e D[c_\sigma^B - c_\sigma^A]} = \int_E \frac{\mp 1}{\pi^2} \frac{\partial \gamma_\sigma}{\partial \zeta}(\xi, 0, \tau) d\xi \tag{8}$$

where minus or plus signs should be used when the species σ corresponds to O or R respectively.

Since this work deals with simulations of a cell which includes a counter electrode near the IDAE, the conventional assumptions of large number of bands and far counter electrode were discarded. Therefore, $N_B = N_A + 1 = 4$ was considered, which is a sufficiently small number of bands. Additionally, the location of the counter electrode was forced close to the IDAE by choosing its separation from the IDAE to be $w_G = W$. The total width of the counter electrode (left and right parts together) was chosen equal to the width of the IDAE, which facilitates the verification of the results obtained by simulations. Also, arrays with bands of equal widths and gaps ($w_A = w_B = W/2$) were considered for all simulations, which is a common design choice.

For simplicity, a mesh with shape of uniform grid was chosen for all simulations. This mesh consisted of $n_x \times n_z$ elements, where the size of each element was $\delta_x = \delta_z = \delta$. The resolution of the mesh was tested for the case of steady-state diffusion where the cell has an aspect ratio of $H/W = 1$. The resolution was successively refined until the absolute error of the normalized current between two consecutive iterations was less than 0.005, which corresponds approximately to two decimal places of accuracy. The value obtained for the element size was $\delta = 0.01$, and was used for all simulations in this work.

All simulations were solved numerically by writing the normalized diffusion equation, its boundary conditions and the corresponding meshes in Python with the aid of the package FiPy [12]. The implementations of such simulations can be downloaded from [13].

Verification of the simulation's implementation

The fact that the counter electrode and the IDAE have equal widths facilitates the estimation of the concentration at the counter electrode, since from Eq. (4) one must have

$$\left[\gamma_{\sigma}^{\mathrm{IDAE}} - \gamma_{\sigma,i}\right] + \left[\gamma_{\sigma}^{C} - \gamma_{\sigma,i}\right] \approx 0 \tag{9}$$

where $\gamma_{\sigma}^{\mathrm{IDAE}} = 1/2$ is the normalized version of the average concentration on the IDAE, γ_{σ}^{C} is the normalized concentration on the counter electrode, and $\gamma_{\sigma,i}$ is the normalized initial concentration in the cell. This relation holds only approximately, since it does not take into account the average concentration at the gap between the IDAE and the counter electrode. The average concentration in this gap is in general different from the initial concentration in the cell, however its effect on Eq. (9) can be reduced when its width w_G is small.

To verify the correct implementation of the simulations, as well as the boundary condition at the counter electrode, we numerically solved the concentration profile for two cases of initial concentration: (i) The case $\gamma_{\sigma}^{\mathrm{IDAE}} = \gamma_{\sigma,i} = 1/2$, where the average concentration applied to the arrays equals the initial concentration. This condition must produce a concentration on the counter electrode of $\gamma_{\sigma}^{C} \approx 1/2$, since this is required to maintain the average concentration in the cell equal to $\gamma_{\sigma,i} = 1/2$ while the average concentration on the IDAE is $\gamma_{\sigma}^{\mathrm{IDAE}} = 1/2$. (ii) The case $\gamma_{\sigma}^{\mathrm{IDAE}} > \gamma_{\sigma,i} = 1/4$, where the average concentration on the IDAE is greater than the initial concentration in the cell. This condition must produce a concentration on the counter electrode of $\gamma_{\sigma}^{C} \approx 0$ in order to maintain the average concentration in the cell equal to $\gamma_{\sigma,i} = 1/4$ while the average concentration on the IDAE is $\gamma_{\sigma}^{\mathrm{IDAE}} = 1/2$.

Steady-state currents and collection efficiencies in terms of cell height

After verifying the implementation of the simulations, steady-state currents and collection efficiencies for cells of different heights were obtained by solving the steady-state diffusion equation numerically. The relative heights (aspect ratios) used in the simulations were $H/W = \{1, 1/2, 1/3, \ldots, 1/10\}$. The normalized currents obtained for the arrays *A* and *B* were taken to compute collection efficiencies, which correspond to the ratio between the currents collected and generated at the IDAE. Due to the boundary conditions in Eqs. (7c, d), the array *A* corresponds to the collector, while the array *B,* to the generator.

RESULT AND DISCUSSION

Verification of implementation for the case $\gamma_{\sigma}^{IDAE} = \gamma_{\sigma,i} = 1/2$

This case corresponds to the situation in which the initial concentration in the cell and the average concentration applied on the IDAE are equal. Figure 2 shows that the bipotentiostat effectively adjusts the concentration at the counter electrode to the predicted value $\gamma_{\sigma}^{C} \approx 1/2$, in order to maintain the average concentration in the cell equal to $\gamma_{\sigma,i} = 1/2$, while the average concentration applied at the IDAE remains at $\gamma_{\sigma}^{\mathrm{IDAE}} = 1/2$. In this case γ_{σ}^{C} is not exactly 1/2, because the average concentration in the gap between the IDAE and the counter electrode is slightly different from 1/2.

Figure 2 also shows that the concentration profile near the left side of the simulation domain (the center of the full cell) presents units of symmetry arranged in a periodic fashion. However, near the ends of the IDAE, this symmetry is lost due to the close proximity of the counter electrode.

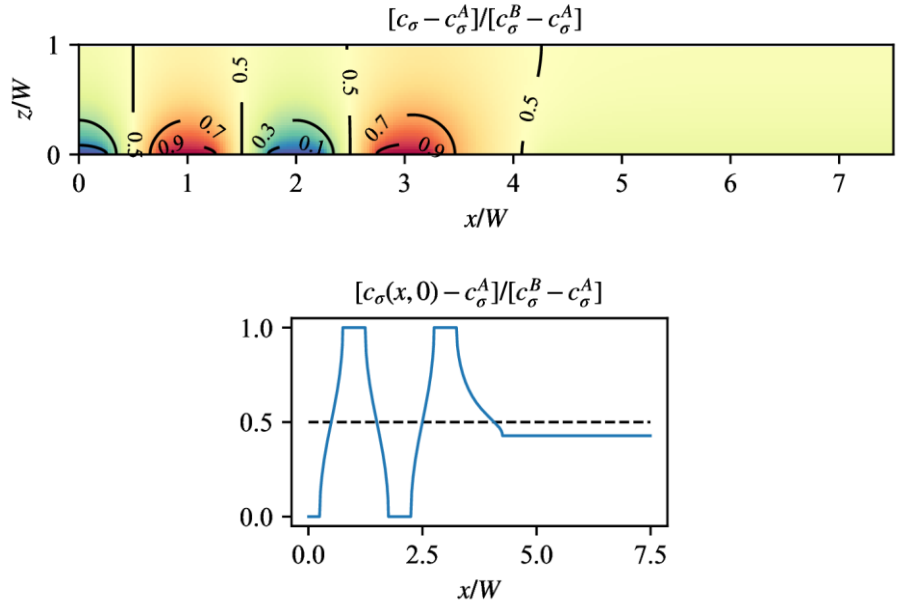

Figure 2. Normalized concentration in steady state (in the whole cell and at the bottom of the cell) when the initial concentration of the species equals $\gamma_{\sigma,i} = 1/2$ ($c_{\sigma,i} = c_\sigma^B/2 + c_\sigma^A/2$). Here the average concentration at the IDAE is $\gamma_\sigma^{\mathrm{IDAE}} = 1/2$ ($c_\sigma^{\mathrm{IDAE}} = c_\sigma^B/2 + c_\sigma^A/2$), therefore the concentration at the counter electrode must be $\gamma_\sigma^C \approx 1/2$ ($c_\sigma^C \approx c_\sigma^B/2 + c_\sigma^A/2$) in order to maintain the average of the cell at $\gamma_{\sigma,i} = 1/2$.

Since the counter electrode is close to the IDAE, the current at the counter electrode is non-zero (Figure 3). This is because some of the electrochemical species generated at the array *B* cannot be collected by the array *A*, and escapes by diffusion to the region of bulk concentration of the cell, and finally travels to the counter electrode. The normalized currents obtained in steady state at the arrays *A* and *B* were –0.30 and 0.38 respectively, while that at the counter electrode was –0.08. This translates into a collection efficiency of $|i_A/i_B| \approx 0.80 = 80\%$.

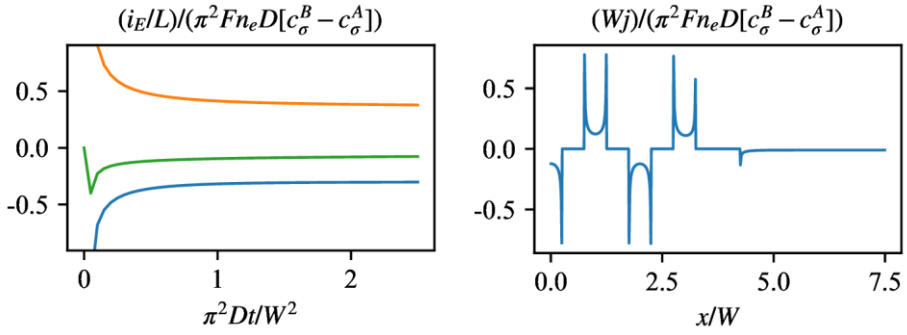

Figure 3. Time response of the normalized current (left) at the array *A* (blue), array *B* (orange) and counter electrode *C* (green), and normalized current density in steady state at the bottom of the cell (right), when the initial concentration of the species equals $\gamma_{\sigma,i} = 1/2$ ($c_{\sigma,i} = c_\sigma^B/2 + c_\sigma^A/2$).

Verification of implementation for the case $\gamma_\sigma^{IDAE} > \gamma_{\sigma,i} = 1/4$

In this case, the average concentration on the IDAE is higher than the average concentration in the cell. Consequently, Figure 4 shows that the bipotentiostat can adjust the concentration on the counter electrode to the predicted value $\gamma_\sigma^C \approx 0$, thus mantaining the average concentration in the cell equal to $\gamma_{\sigma,i} = 1/4$ while the average concentration at the IDAE remains at $\gamma_\sigma^{IDAE} = 1/2$.

Comparing with the previous case ($\gamma_\sigma^{IDAE} = \gamma_{\sigma,i}$), once the average concentration on the IDAE is increased above the average concentration in the cell ($\gamma_\sigma^{IDAE} > \gamma_{\sigma,i}$), the concentration on the counter electrode is automatically adjusted to decrease below the average concentration in the cell ($\gamma_\sigma^C < \gamma_{\sigma,i}$). This adjustment occurs in the same proportion for the IDAE and the counter electrode (but in opposite directions) according to Eq. (9), since the widths of the IDAE and counter electrode are equal. However, the concentration on the counter electrode cannot decrease indefinitely, and must stop decreasing when $\gamma_\sigma^C \approx 0$. This corresponds to the the case when the currents generated at the IDAE and at the counter electrode are maximum.

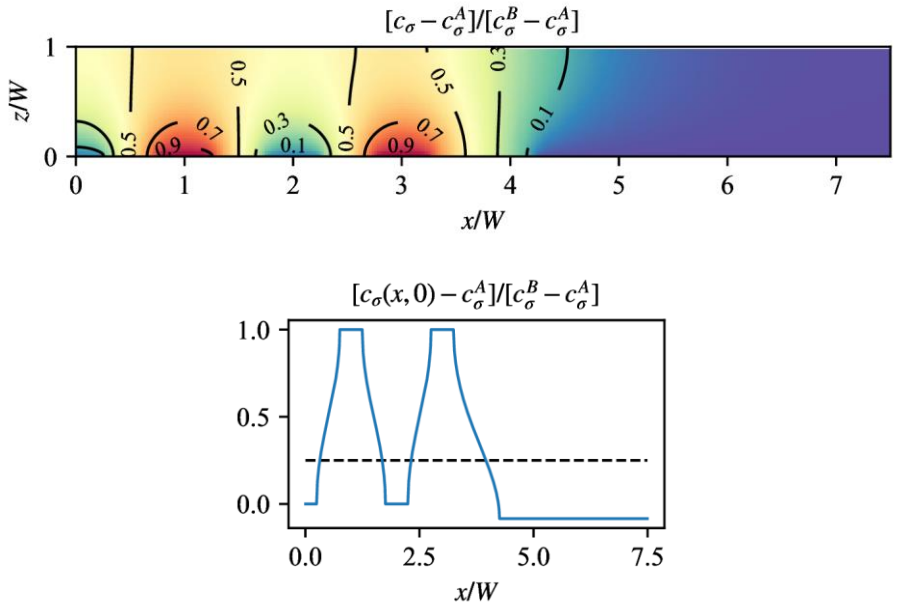

Figure 4. Normalized concentration in steady state (in the whole cell and at the bottom of the cell) when the initial concentration of the species equals $\gamma_{\sigma,i} = 1/4$ ($c_{\sigma,i} = c_\sigma^B/4 + 3c_\sigma^A/4$). Here the average concentration at the IDAE is $\gamma_\sigma^{IDAE} \approx 1/2$ ($c_\sigma^{IDAE} \approx c_\sigma^B/2 + c_\sigma^A/2$), therefore the concentration at the counter electrode must be $\gamma_\sigma^C \approx 0$ ($c_\sigma^C \approx c_\sigma^A$) in order to maintain the average of the cell at $\gamma_{\sigma,i} = 1/4$.

Figure 5 shows that the currents at the array *A*, array *B* and the counter electrode reach steady-state values of approximately –0.30, 0.40 and –0.10, which translates into a collection efficiency of $|i_A/i_B| \approx 0.74 = 74\%$. These currents are higher than those of the previous case (–0.30, 0.38 and –0.08 respectively), while the collection efficiency in this case is lower than that of the previous case (≈ 80%). These maximum currents are related to the gradient of concentration existing in between the IDAE and the counter electrode (Figure 4), which is clearly stronger than that in Figure 2.

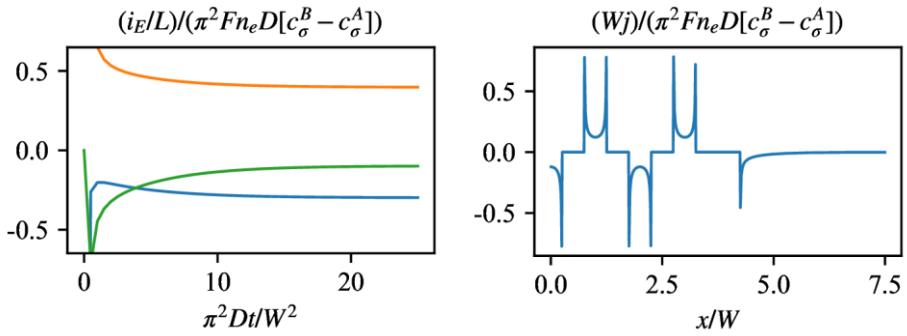

Figure 5. Time response of the normalized currents (left) at the array *A* (blue), array *B* (orange) and counter electrode *C* (green), and normalized current density in steady state at the bottom of the cell (right), when the initial concentration of the species equals $\gamma_{\sigma,i} = 1/4$ ($c_{\sigma,i} = c_\sigma^B/4 + 3c_\sigma^A/4$).

Steady-state currents and collection efficiencies in terms of cell height

In this section we focus only on the case where the IDAE generates the maximum current possible, that is, when $\gamma_{\sigma,i} = 1/4$. For this case we are interested on how the steady-state currents and the collection efficiency vary as the electrochemical cell becomes shallower.

Figure 6 shows that the steady-state currents on all electrodes decrease as the cell becomes shallower. This has its explanation in the number of gradients present in the concentration profile (Figure 4). There is one gradient between the IDAE and the roof of the cell, other gradient between consecutive bands of the IDAE, and another between the IDAE and the counter electrode. All these gradients contribute to the currents at the electrodes. However, as the cell becomes shallower, the gradient between the IDAE and the roof of the cell tends to disappear, leaving only two remaining gradients, which reduces the magnitude of the currents at the different electrodes.

Figure 6 also shows that the collection efficiency in steady state increases as the cell becomes shallower. This also can be explained by looking at the concentration profile in the cell (Figure 4). When the cell is still tall, some of the species generated at the array *B* cannot be collected by the array *A*, thus escaping to the region of bulk concentration near the roof of the cell, and finally reaching the counter electrode. However, when the cell becomes shallower, the lower roof of the cell forces the species generated at the array *B* to be collected at the array *A*, preventing the species to reach the counter electrode outside the IDAE.

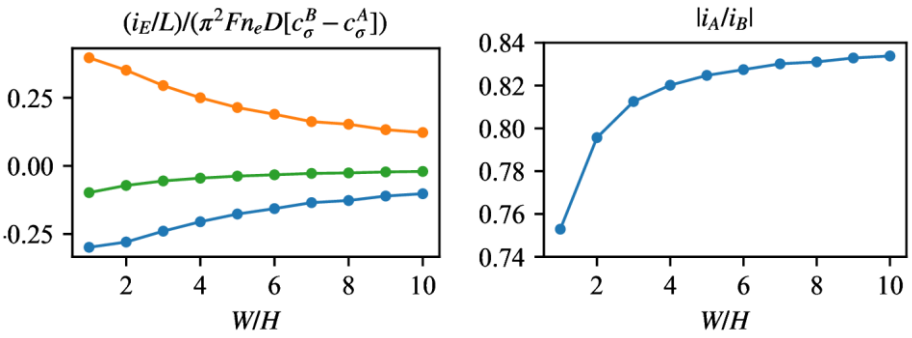

Figure 6. Normalized current in steady state (left) at the array *A* (blue), array *B* (orange) and counter electrode *C* (green), and collection efficiency (right) for different values of *W*/*H*. All simulations considered initial concentration of $\gamma_{\sigma,i} = 1/4$, which corresponds to the case of maximum currents in the IDAE.

Both phenomena indicate that there are compromised design criteria when choosing the height of the electrochemical cell: As the cell becomes shallower, lower sensitivity of the electrochemical sensor is obtained (in terms of current), while the performance of the IDAE improves (in terms of collection efficiency). This means that higher currents can be obtained at the expense of lower collection efficiency when the cell is tall, while higher collection efficiency can be obtained at the expense of lower currents when the cell is shallow.

CONCLUSION

The key question of this work, whether it is possible to simulate an electrochemical cell containing an IDAE and a counter electrode in close proximity has been addressed. The main problem that makes this sort of simulation difficult is that the potential (and the concentrations) at the counter electrode are not known before performing an experiment or simulation. However, this problem can be addressed by using an additional property, which states that the average concentration in the cell is constant when Kirchhoff's current law is satisfied in the cell. This corresponds to a specialized form of the continuity equation for the amount of species in the cell, and allows to obtain the missing concentration at the counter electrode.

The property of constant average concentration in the cell also allows to obtain rough estimations of what the concentration at the counter electrode would be. In particular, if the widths of the IDAE and the counter electrode are equal, the change in concentration at the counter electrode with respect to the initial concentration in the cell is equal and opposite to the change in average concentration at the IDAE. This helped to roughly predict the concentration at the counter electrode before performing the simulations, in order to validate them.

If the concentration on the counter electrode decreases as the average concentration on the IDAE increases, there is a point when the concentration at the counter electrode reaches zero, and therefore cannot decrease further. It is at this point where the gradients of concentration in the cell are maximum, and therefore the steady-state currents produced are also maximum.

If we produce maximum steady-state currents, but we change the height of the cell, the magnitude of the steady-state currents and the collection efficiencies are affected. As the cell becomes shallower, lower steady-state currents and higher collection efficiencies are obtained. This indicates the existence of trade-offs between sensitivity (in terms of current) and performance (in terms of collection efficiency) of the sensor. Higher currents can be traded by lower collection efficiencies when the cell is tall, and higher collection efficiencies can be traded by lower currents when the cell is shallow.

ACKNOWLEDGEMENT

The authors gratefully acknowledge *Petchra Pra Jom Klao Ph.D. Scholarship* (Grant No. 28/2558), *King Mongkut's University of Technology Thonburi.* The authors also acknowledge the financial support provided by *King Mongkut's University of Technology Thonburi* and the *Research Network NANOTEC* (RNN) program (Grant No. P1851883) of the *National Nanotechnology Center* (NANOTEC), NSTDA, Ministry of Science and Technology, Thailand.

REFERENCES

[1] Karimian, N. and Ugo, P. Recent advances in sensing and biosensing with arrays of nanoelectrodes. *Current Opinion in Electrochemistry*. 2019; 16: 106 – 116.
[2] Rackus, D. G.; Shamsi, M. H. and Wheeler, A. R. Electrochemistry, biosensors and microfluidics: A convergence of fields. *Chemical Society Reviews*. 2015: 44: 5320 – 5340.
[3] Gencoglu, A. and Minerick, A. R. Electrochemical detection techniques in micro- and nanofluidic devices. *Microfluidics and Nanofluidics*. 2014; 17: 781 – 807.
[4] Strutwolf, J. and Williams, D. E. Electrochemical sensor design using coplanar and elevated interdigitated array electrodes. A computational study. *Electroanalysis*. 2015; 17 (2): 169 – 177.
[5] Morf, W. E.; Koudelka-Hep, M.; de Rooij, N. F. Theoretical treatment and computer simulation of microelectrode arrays. *Journal of Electroanalytical Chemistry*. 2006; 590: 47 – 56.
[6] Kanno, Y.; Goto, T.; Ino, K.; Inoue, K. Y.; Takahashi, Y.; Shiku, H. and Matsue, T. SU-8-based Flexible Amperometric Device with IDA Electrodes to Regenerate Redox Species in Small Spaces. *Analytical Sciences*. 2014; 30: 305 – 309.
[7] Heo, J.-I.; Lim, Y. and Shin, H. The effect of channel height and electrode aspect ratio on redox cycling at carbon interdigitated array nanoelectrodes confined in a microchannel. *Analyst*. 2013; 138: 6404 – 6411.
[8] Aoki, K.; Morita, M.; Niwa, O. and Tabei, H. Quantitative analysis of reversible diffusion-controlled currents of redox soluble species at interdigitatedgitated array electrodes under steady-state conditions. *Journal of Electroanalytical Chemistry and Interfacial Electrochemistry*. 1988; 256: 269 – 282.
[9] Yu, Y.-H. Microfabrication of a digital microfluidic platform integrated with an on-chip electrochemical cell. *Journal of Micromechanics and Microengineering*. 2013; 23 (9): 095025.
[10] Guajardo, C.; Ngamchana, S. and Surareungchai, W. Mathematical modeling of interdigitated electrode arrays in finite electrochemical cells. *Journal of Electroanalytical Chemistry*. 2013; 705: 19 – 29.
[11] Oldham, K and Myland, J. Fundamentals of electrochemical science. 1st Edition. Elsevier, 1994, 447.
[12] Guyer, J. E.; Wheeler, D. and Warren, J. A. FiPy: Partial differential equations with Python. Computing in Science and Engineering; 2009. DOI: 10.1109/MCSE.2009.52
[13] Guajardo Yévenes, Cristian F. *Simulation of interdigitated array of electrodes with counter electrode in shallow electrochemical cell using FiPy*. 31 October 2021; https://doi.org/10.5281/zenodo.5633334